Journal of Catalysis 267 (2009) 57–66

Contents lists available at ScienceDirect

Journal of Catalysis

journal homepage: www.elsevier.com/locate/jcat

Effects of alkali promotion of TiO_2 on the chemisorptive properties and water–gas shift activity of supported noble metal catalysts

Paraskevi Panagiotopoulou, Dimitris I. Kondarides *

Department of Chemical Engineering, University of Patras, GR-26504 Patras, Greece

ARTICLE INFO

Article history:
Received 9 April 2009
Revised 26 July 2009
Accepted 28 July 2009
Available online 2 September 2009

Keywords:
Water–gas shift
Noble metal
Titanium dioxide
Oxygen vacancy
Alkali
Promotion
TPD
Kinetic measurements
Metal-support interactions
SMSI effect

ABSTRACT

The effects of alkali promotion of TiO_2 on the chemisorptive properties and water–gas shift (WGS) activity of dispersed noble metal catalysts (NM = Pt, Ru, Pd) have been investigated over NM/X–TiO_2 samples of variable promoter type (X = Li, Na, K, Cs) and loading (0.0 to 0.68 wt.%). Results of H_2-TPD experiments show that addition of alkalis does not affect appreciably the population and chemisorption strength of hydrogen adsorbed on the surface of dispersed metal crystallites indicating that these sites are not influenced by the presence of the promoter. In contrast, the desorption temperature of hydrogen adsorbed on sites located at the metal-support interface shifts monotonically toward lower temperatures with increasing alkali content. This has been attributed to alkali-induced reduction of Ti^{4+} surface species and creation of a new type of sites at the perimeter of the dispersed metal crystallites, which are in contact with the support. These sites are of the form of NM–$\square_s$–Ti^{3+}, where $\square_s$ denotes an oxygen defect vacancy, and provide the necessary dual-function sites required for the WGS reaction to proceed. Catalytic performance tests and kinetic measurements show that activity depends appreciably on the nature and loading of added alkali, whereas the apparent activation energy (E_a) of the reaction does not vary to a large extent. For Pt/X–TiO_2 catalysts, a volcano-type dependence of intrinsic reaction rate on the chemisorption strength of Pt–$\square_s$–Ti^{3+} sites toward hydrogen has been found to exist. Optimized catalysts are about three times more active than unpromoted Pt/TiO_2. Results are discussed with respect to the alkali-induced modifications of the physicochemical properties of the support on the population, chemisorptive properties, and catalytic activity of sites located at the metal-support interface.

1. Introduction

Chemical [1–11] or electrochemical [12–17] promotion of catalytic materials by alkalis has been the subject of several recent investigations. The origin of the continued interest in this topic is both of fundamental and applied nature. Alkali additives are known to enhance the rate of many industrially important catalytic reactions, such as ammonia and Fisher–Tropsch syntheses [18], and can be also used to study the effects of promoters on the chemisorptive and catalytic properties of materials. Examples of alkali-promoted catalytic reactions investigated in the past few years include selective catalytic reduction of NO by CO or hydrocarbons in the absence [1,2] or in the presence [6,13,14] of oxygen, oxidation of NO [4], ethylene epoxidation [15], deep oxidation of ethanol [5] and hydrocarbons [16], oxidation [17] and preferential oxidation [6,7] of carbon monoxide, CO hydrogenation [8,9] and water–gas shift reaction [10,11]. Results of these studies clearly show that alkalis induce a strong promotional effect on the performance of metal catalysts, which is often reflected in enhanced activity, higher selectivity, suppression of undesirable reactions, and/or improvement of catalyst stability [1–17]. The ability of alkali additives to modify catalytic performance can be understood by considering the geometric and electronic-type effects induced by the promoting species on the chemisorptive properties of metal surfaces toward reactive molecules [19,20]. Regarding the latter type of interactions, alkali metals are electron donors and, when present on the surface of a metal catalyst, may act by enhancing chemisorption of electron acceptor species, such as carbon monoxide and oxygen, and/or by suppressing chemisorption of electron donors, such as olefins and hydrogen [12].

Water–gas shift ($CO + H_2O \leftrightarrow CO_2 + H_2$) is a suitable reaction for studying the effects of promoters on catalytic performance because it involves simple molecules, namely, carbon monoxide and hydrogen, which can be easily probed with a variety of techniques. In addition, the reaction is of significant practical importance, mainly due to the recent efforts for developing fuel processors capable of converting carbonaceous fuels into hydrogen for fuel cell applications [21].

In our previous studies [22–26], we have investigated in detail the WGS activity of noble metal catalysts (Pt, Rh, Ru, Pd) dispersed

* Corresponding author. Fax: +30 2610 991527.
E-mail address: dimi@chemeng.upatras.gr (D.I. Kondarides).

0021-9517/$ - see front matter © 2009 Elsevier Inc. All rights reserved.
doi:10.1016/j.jcat.2009.07.014

on a variety of metal oxide supports. It has been found that Pt is generally much more active than Pd, with Rh and Ru exhibiting an intermediate performance [22]. It was also shown that noble metals supported on reducible metal oxides, such as TiO_2 [22–24] and CeO_2 [23–25], are characterized by higher activity for the WGS reaction than catalysts supported on irreducible oxides, such as Al_2O_3 or SiO_2 [23,24], and that activity generally increases with decreasing primary particle size of the support [22,24,26]. In our recent investigation [27], it was shown that addition of Na or Cs on Pt/TiO_2 catalyst results in the creation of new sites with increased electron density, proposed to be located at the metal-support interface. The adsorption strength of these sites toward CO was found to increase with increase of alkali content, whereas the opposite was found to be true for adsorption of hydrogen [27]. The aim of the present study is to investigate the promoting effects of alkalis (Li, Na, K, Cs) on the WGS activity of NM/TiO_2 catalysts (NM = Pt, Ru, Pd) and to correlate catalytic performance with the alkali-induced alterations of the physicochemical properties of the support and of the chemisorptive properties of dispersed noble metal crystallites.

2. Experimental

2.1. Catalyst preparation and characterization

Alkali-promoted TiO_2 supports, denoted in the following as X–TiO_2 (X = Li, Na, K, Cs), were prepared by impregnation of titanium dioxide powder (Degussa P25) with an aqueous solution containing the appropriate amount of Li_2CO_3, $NaNO_3$, KNO_3, or $CsNO_3$. This was followed by drying at 110 °C overnight and calcination in air at 600 °C for 3 h [27]. Dispersed noble metal catalysts (NM = Pt, Ru, Pd) were prepared employing the wet impregnation method with the use of $(NH_3)_2Pt(NO_2)_2$, $Ru(NO)(NO_3)_3$, or $(NH_3)_2Pd(NO_2)_2$ (Alfa) as metal precursor salts and the above X–TiO_2 powders as supports [22,27]. The solid residue was dried at 110 °C for 24 h and then reduced at 300 °C (400 °C for Ru catalysts) in H_2 flow for 2 h. The nominal metal loading of all catalysts thus prepared was 0.5 wt%.

Specific surface area (SSA) of catalytic materials was measured employing nitrogen physisorption at the temperature of liquid nitrogen (B.E.T. method). Noble metal dispersion (D_{NM}) and mean crystallite size (d_{NM}) were estimated by selective chemisorption of CO (H_2 for Ru catalysts). The anatase-to-rutile content of TiO_2 was determined with the use of X-ray diffraction (XRD). Details on the apparatuses, methods, and procedures used for catalyst characterization can be found elsewhere [22].

Temperature-programmed desorption (TPD) experiments were carried out over freshly prepared catalysts as described in detail elsewhere [27]. Briefly, an amount of catalyst (200 mg) was reduced *in situ* with hydrogen at 300 °C, purged with He at 500 °C to remove adsorbed species from the catalyst surface, and then cooled down to 25 °C under He flow. This was followed by adsorption of H_2 at 25 °C for 15 min, purging with He for 10 min, and linear increase of temperature (β = 30 °C min^{-1}) to 650 °C under He flow (40 cm^3 min^{-1}). A mass spectrometer (Omnistar, Pfeiffer Vacuum) was used for on-line monitoring of the TPD patterns.

2.2. Catalytic performance tests and kinetic measurements

The catalytic performance of the synthesized materials for the WGS reaction was investigated in the temperature range of 100 to 500 °C, using a feed stream consisting of 3% CO and 10% H_2O (balance He). The mass of catalyst used in these experiments was typically 100 mg (particle size: $0.18 < d_p < 0.25$ mm) and the total flow rate was 200 cm^3 min^{-1}. Prior to each experiment the catalyst was reduced *in situ* at 300 °C for 1 h under a hydrogen flow of 60 cm^3 min^{-1}. The catalyst was then heated at 500 °C under He flow, left at that temperature for 15 min, and finally conditioned by exposure to the reaction mixture at 450 °C for 1 h. Concentrations of reactants and products were determined at steady-state conditions using the analysis system described above. Similar measurements were obtained following a stepwise lowering of temperature, until conversion of CO dropped close to zero. All experiments were performed at near atmospheric pressure.

Measurements of intrinsic reaction rates were obtained in separate experiments under differential reaction conditions, where the conversion of reactants was kept below 10%. Results were used to determine the turnover frequency (TOF) of carbon monoxide, defined as moles of CO converted per surface noble metal atom per second. Details on the methods and procedures employed can be found elsewhere [22].

3. Results

3.1. Catalyst characterization

In Table 1 are summarized results of physicochemical characterization of the synthesized materials. It is observed that specific surface area (SSA) is practically the same for all catalysts investigated (25 to 30 m^2 g^{-1}), indicating that this parameter is not influenced by addition of small amounts of alkalis on the support. The same is true for the primary crystallite size of TiO_2, determined by X-ray line broadening, which was found to vary in the range of 20 to 26 nm. Regarding the anatase content of the support, it is generally higher for alkali-promoted samples than bare TiO_2 (Table 1). It should be noted, however, that both SSA and anatase content are substantially lower than those of the parent TiO_2 material (48 m^2 g^{-1}, 75% anatase). This is because synthesis included heat treatment at elevated temperature (600 °C for 3 h), which is known to result in transformation of TiO_2 to its rutile form, particle growth, and decrease in specific surface area [27].

Regarding metal dispersion, results presented in Table 1 show that platinum is well dispersed for all $Pt/X–TiO_2$ samples investigated, with the average size of Pt crystallites ranging between 1.0 and 1.5 nm. Dispersion of Ru and Pd catalysts is relatively lower, and the corresponding mean crystallite sizes vary in the ranges of 1.4 to 2.3 nm and 1.7 to 2.4 nm, respectively (Table 1).

3.2. Temperature-programmed desorption of H_2

3.2.1. Pt catalysts

Results of H_2-TPD experiments obtained over bare and alkali-promoted Pt/TiO_2 catalysts of the same dopant loading (alkali:Pt atomic ratio = 1:1) are presented in Fig. 1. It is observed that hydrogen desorbs from the unpromoted sample (trace a) exhibiting three peaks centered at *ca.* 115, 285, and 350 °C. As has been discussed in detail in our previous study [27], the low temperature (LT) peak is due to hydrogen chemisorbed on the surface of Pt crystallites [28–30], whereas the high temperature (HT) feature can be attributed to spillover hydrogen associated with the support [29,31]. The medium temperature (MT) peak has been assigned to hydrogen adsorbed on sites located at the periphery of Pt crystallites, which are in contact with the TiO_2 support [27]. This assignment is in agreement with previous work obtained over Pt/LTL zeolite catalysts [31] and over Rh catalysts supported on Al_2O_3 or CeO_2 [32,33], which indicated the presence of new adsorption sites at the metal-support interface.

Addition of alkalis (traces b–e) does not affect appreciably the intensity or position of the LT peak, indicating that adsorption sites located on the surface of Pt crystallites are not influenced by the presence of the promoters. This finding, which is supported by

Table 1
Physicochemical characteristics of synthesized NM/X–TiO_2 catalysts and representative results of kinetic measurements.

Dispersed metal catalyst (0.5 wt.%)	Promoter type and nominal loading (wt.%)		Alkali:NM atomic ratio (nominal)	SSA ($m^2\ g^{-1}$)	Anatase content (%)	Noble metal dispersion	d_{NM} (Å)	Rate at 250 °C		E_a (kJ mol^{-1})
								(μmol $s^{-1}\ g^{-1}$)	TOF (s^{-1})	
Pt	None	0	0.0	29	48	0.87	12	10.3	0.51	66
	Li	0.018	1.0	25	36	0.89	11	28.9	1.27	76
	Na	0.017	0.3	30	52	0.94	11	18.1	0.76	63
		0.06	1.0	27	56	1.01	10	38.4	1.58	71
		0.12	2.0	28	50	0.66	15	23.4	1.35	69
		0.20	3.4	28	56	0.81	13	22.3	1.07	72
	K	0.10	1.0	30	55	0.71	14	26.7	1.47	63
	Cs	0.17	0.5	30	50	0.78	13	16.9	0.86	69
		0.34	1.0	28	48	0.77	13	23.6	1.19	68
		0.68	2.0	28	59	0.74	14	7.75	0.40	68
Ru	None	0	0.0	29	48	0.46	21	1.56	0.07	66
	Na	0.06	0.5	27	56	0.70	14	5.87	0.17	52
		0.20	1.8	28	56	0.42	23	6.40	0.30	49
Pd	None	0	0.0	29	48	0.67	17	0.82	0.03	72
	Cs	0.34	0.5	28	48	0.47	24	2.29	0.10	62
		0.68	1.1	28	59	0.54	21	1.30	0.05	60

results of our recent FTIR experiments using CO as probe molecule [27], implies that alkali atoms are mainly located on the TiO_2 support. It should be noted that the synthesis method employed here involves addition of alkali on TiO_2 prior to dispersion of noble metals. As will be discussed below, the added alkalis interact strongly with the support and this probably hinders diffusion of promoter atoms to the surface of dispersed metal crystallites. The HT shoulder decreases in intensity in the presence of alkalis as a result of alkali-induced dehydroxylation of the support, which is known to suppress spillover of hydrogen [7,27,31]. Regarding the MT peak, it shifts from 285 °C for the unpromoted catalyst to *ca.* 245 °C for samples promoted with Li, K, or Cs and to 260 °C for the catalyst promoted with Na (Fig. 1). This implies that the adsorption strength of the corresponding sites toward hydrogen decreases significantly in the presence of the promoters. Thus, it seems that the effect of alkali on the chemisorptive properties of platinum is of short-range, i.e., it is restricted to metal sites located in the close vicinity of the alkali-promoted TiO_2 support.

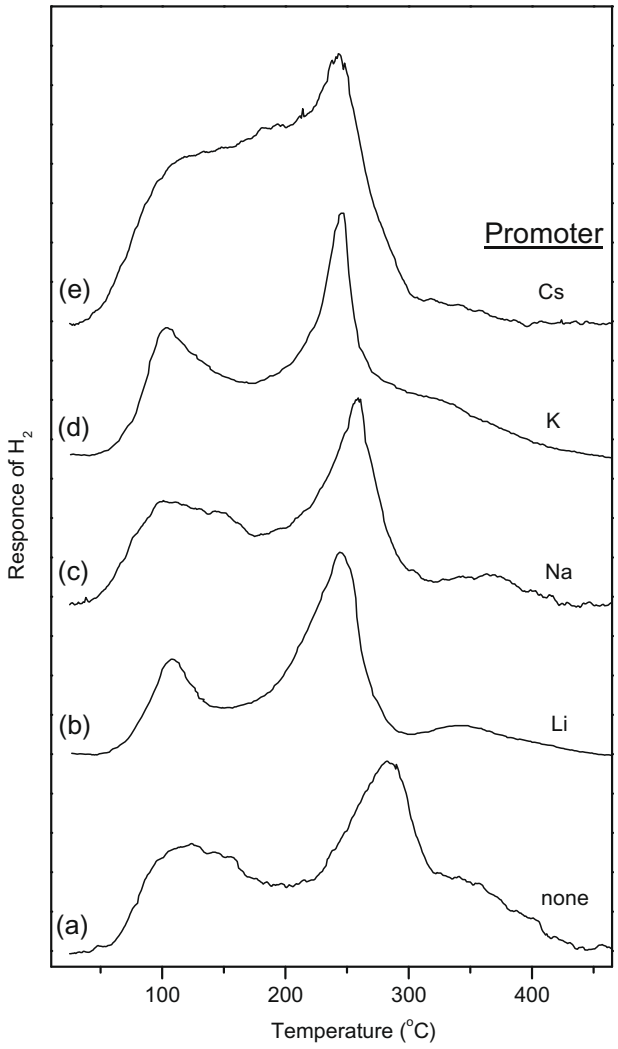

Fig. 1. Temperature-programmed desorption profiles obtained over Pt/TiO_2 and $Pt/X–TiO_2$ (X = Li, Na, K, Cs) catalysts of the same alkali:Pt atomic ratio (X:Pt = 1:1) following adsorption of hydrogen at 25 °C for 15 min.

Similar H_2-TPD experiments conducted over catalysts promoted with variable amounts of Na (0 to 0.20 wt.%) or Cs (0 to 0.68 wt.%) showed that the downward shift of the MT peak increases with increasing alkali content [27]. Results obtained for all $Pt/X–TiO_2$ catalyst samples investigated in our previous [27] and in the present study are summarized in Fig. 2, where the temperature at which the maximum of the MT peak is observed (T_{max}) is plotted as function of alkali:Pt atomic ratio. It is observed that T_{max} decreases monotonically with increasing alkali content, and that the effect is more pronounced for Cs-doped than Na-doped samples of the same alkali:Pt ratio. As will be discussed below, the presence of electropositive alkali atoms in the vicinity Pt sites located at the metal-support interface results in the creation of sites of higher electron-donating properties and, therefore, of weaker Pt–H bond strength. It should be noted that the opposite is true for adsorption of CO, which is an electron acceptor molecule. In fact, our recent FTIR results have shown that addition of alkali results in a red shift of the ν(CO) stretching frequency of species adsorbed on these sites, which implies strengthening of the Pt–CO bond with increasing alkali content [27].

3.2.2. Pd and Ru catalysts

In order to investigate if the effect of alkali promotion on hydrogen adsorption/desorption characteristics is operable for noble metal catalysts other than platinum, H_2-TPD experiments were also conducted for Pd and Ru dispersed on representative $X–TiO_2$ supports. Results obtained over $Pd/Cs–TiO_2$ and $Ru/Na–TiO_2$ catalysts are depicted in Fig. 3. It is observed that hydrogen desorbs from unpromoted Pd/TiO_2 (Fig. 3A, trace a) exhibiting a LT peak centered

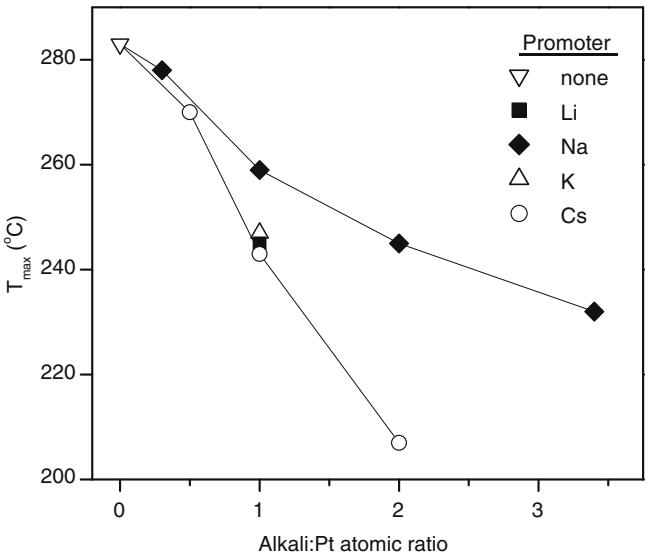

Fig. 2. Effect of alkali:Pt atomic ratio on the desorption temperature (T_{max}) of the medium temperature (MT) hydrogen peak observed in H_2-TPD profiles of Pt/X–TiO_2 catalysts (X = Li, Na, K, Cs).

at *ca.* 100 °C, a MT peak located at 275 °C, and a HT shoulder of much lower intensity above 300 °C. The LT feature is assigned to hydrogen adsorbed on Pd surface [34–36] and may contain a contribution from palladium hydride decomposition [36,37]. The origin of H_2-TPD peaks appearing in the temperature range of 150 to 300 °C is unclear in the literature. Peaks in this region have been often attributed to hydrogen bound to different Pd surface sites, i.e., top, bridge, and multiple coordinated forms on a given surface plane, and/or to hydrogen adsorbed on different Pd planes [34–36]. Following the same reasoning used for Pt/TiO_2 catalysts, we tentatively assign the MT peak located at 275 °C to hydrogen adsorbed at the Pd–TiO_2 interface and the weak HT feature located above 300 °C to spillover hydrogen.

Addition of Cs does not affect, practically, the position and intensity of the LT peak (traces b and c). In contrast, the MT peak exhibits a significant shift toward lower temperatures with increase of Cs content, i.e., from 275 °C over the unpromoted catalyst to 215 and 195 °C for samples with Cs:Pd ratios of 0.5 and 1.1, respectively. The peak intensity increases significantly for low Cs content (trace b) and decreases again for higher dopant loadings (trace c). Qualitatively similar results have been reported by Kazi et al. over Li-promoted Pd/SiO_2 catalysts [8]. The authors found that addition of Li (Li:Pd ratio = 1) resulted in a significant shift of the major H_2 TPD peak from 235 to 160 °C [8]. It was concluded that promotion by Li decreases the strength of hydrogen adsorption and increases the strength of CO adsorption on Pd/SiO_2 [8].

The TPD pattern obtained for the Ru/TiO_2 catalyst is characterized by two peaks located at *ca.* 110 and 260 °C (Fig. 3B, trace a). As in the case of Pt and Pd catalysts, the LT peak can be assigned to hydrogen desorption from Ru metal, and the MT peak to hydrogen originating from the metal-support interface. Qualitatively similar TPD patterns have been reported by Lin and Chen [38] over Ru catalysts dispersed on TiO_2, Al_2O_3, and SiO_2 where, depending on the nature of the support, the LT peak was centered at 85 to 125 °C. The authors did not provide an assignment for the MT peak located at around 325 °C for Ru/Al_2O_3 and around 200 °C for Ru/TiO_2. It is of interest to note that the latter peak did not appear over Ru/SiO_2 [38]. As will be discussed below, this is probably expected because creation of sites at the metal-support interface should be less favorable for noble metals dispersed on irreducible supports, such as SiO_2. Regarding the HT peak, which is attributed to spillover hydrogen, it is not discernible over Ru/TiO_2. This is in agreement with results of ESR studies obtained over NM/TiO_2 catalysts [39], which showed that spillover of hydrogen from the metal to the support takes place readily on catalysts containing Pt, Pd, and Rh, but not over Ru/TiO_2.

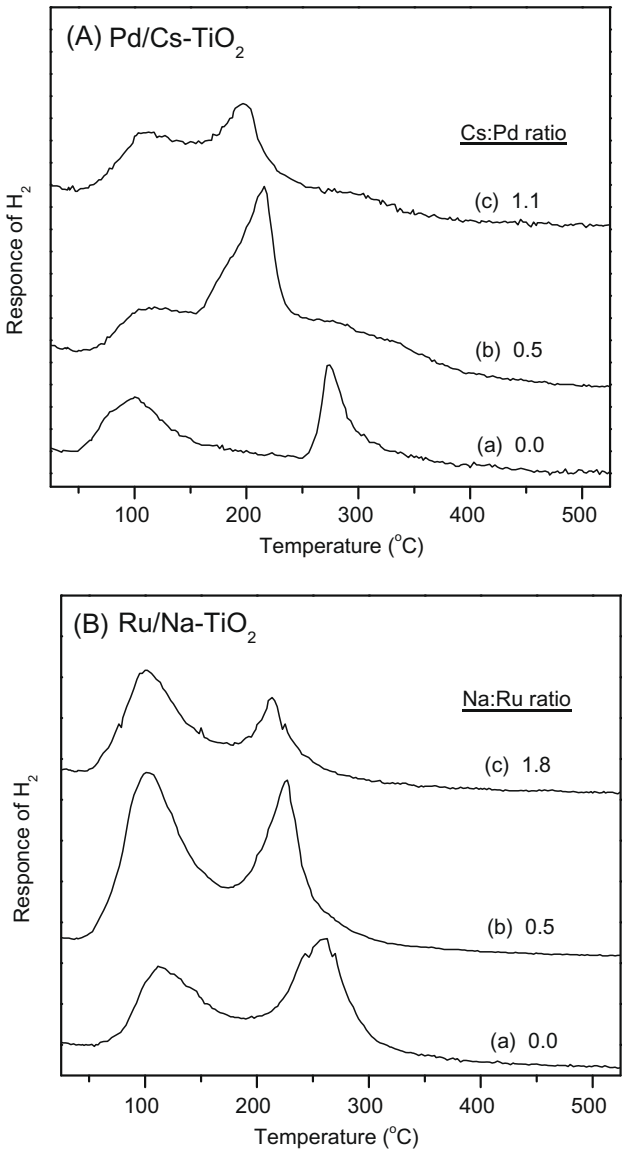

Fig. 3. Temperature-programmed desorption profiles obtained from (A) Cs-promoted Pd/TiO_2 and (B) Na-promoted Ru/TiO_2 catalysts of the indicated alkali loadings.

Addition of 0.06 wt.% Na (Na:Ru = 0.5) to the TiO_2 support results in a significant shift of the MT peak from 245 to 225 °C (trace b), whereas increase of Na loading to 0.20 wt.% (Na:Ru = 1.8) results in a further shift of T_{max} to 215 °C (trace c). This is accompanied by a substantial decrease in the intensity of the MT peak. However, the position of the LT peak is not influenced, practically, by the presence of alkali.

3.3. Catalytic performance tests and kinetic measurements

Resent results obtained over supported platinum catalysts [40–42] showed that freshly prepared Pt/TiO_2 deactivates with time-on-stream under WGS reaction conditions due to loss of Pt

surface area [40]. However, Zhu et al. [42] showed that stability of Pt/TiO_2 can be improved by addition of Na, which was shown to inhibit sintering of Pt crystallites. In the present study, $NM/X–TiO_2$ catalysts were pre-conditioned *in situ* following the procedure described in Section 2.2 (15 min in He flow at 500 °C followed by exposure to the reaction mixture at 450 °C for 1 h). This treatment resulted in materials, which were very stable under the present reaction conditions, with no signs of deactivation.

3.3.1. Pt catalysts

The effects of addition of alkalis on the catalytic performance of Pt/TiO_2 have been investigated over samples promoted with variable amounts of Li, Na, K, or Cs. Results obtained for catalysts of the same alkali:Pt atomic ratio (X:Pt = 1:1) are shown in Fig. 4A, where the conversion of CO (X_{CO}) is plotted as a function of reaction temperature. The equilibrium conversion, predicted by thermodynamics, is also shown for comparison (dashed line). For the unpromoted catalyst, it is observed that X_{CO} becomes measurable at temperatures around 175 °C and increases with increasing temperature until it reaches equilibrium at *ca.* 400 °C. In all cases, addition of alkalis results in a significant shift of the conversion curve toward lower reaction temperatures. This is more pronounced for the Na-promoted sample than samples doped with Li, K, or Cs, which exhibit a similar performance. The Na-promoted catalyst is able to reach equilibrium CO conversion at temperatures around 325 °C, which is about 75 °C lower than that obtained for the unpromoted catalyst. Comparison with the H_2-TPD results obtained over this set of catalysts (Fig. 1) shows that a relation may exist between catalytic performance and the temperature at which the MT peak evolves. In particular, Li-, K-, and Cs-doped catalysts, which exhibit a similar WGS activity (Fig. 4A), are characterized by the same T_{max} for the MT TPD peak (Fig. 1). This issue will be discussed in detail below.

Results of measurements of intrinsic reaction rates, obtained by using low-conversion data exclusively, are summarized in the Arrhenius plots of Fig. 4B. It is observed that the rate (per gram of catalyst) depends on the nature of the promoter and decreases in the order of $Na > Li \approx K \approx Cs > TiO_2$(unpromoted). The same trend is observed for turnover frequencies of CO conversion. Representative results listed in Table 1 show that TOF at 250 °C is more than three times higher for the Na-containing sample than unpromoted Pt/TiO_2. The apparent activation energy (E_a) of the WGS reaction was calculated from the slopes of the fitted lines shown in Fig. 4B and results are summarized in Table 1. It is observed that E_a varies to some extent for this set of catalysts, taking values between 66 and 76 kJ mol^{-1}.

The effect of alkali loading on catalytic performance has been investigated over $Pt/X–TiO_2$ catalysts of variable Na or Cs content, and results obtained are summarized in Fig. 5. For $Pt/Na–TiO_2$ catalysts, it is observed that increasing Na:Pt ratio from 0.0 to 1.0 results in a progressive shift of CO conversion curve toward lower temperatures (Fig. 5A). Further increase of Na content has the opposite effect, as evidenced by the shift of the conversion curve toward higher temperatures. Qualitatively similar results were obtained over $Pt/Cs–TiO_2$ catalysts (Fig. 5B). In particular, increasing Cs:Pt ratio from zero to 1.0 results in a shift of CO conversion curve toward lower temperatures, whereas further increasing Cs content results in catalytic performance similar to that of the unpromoted catalyst. Comparison of results shown in Fig. 5A and B shows that Na catalysts exhibit higher CO conversions at a given temperature than Cs samples of the same alkali:Pt atomic ratio.

Results of reaction rate measurements obtained over the same sets of Na- and Cs-promoted Pt/TiO_2 catalysts are shown in the Arrhenius-type plots of Fig. 6A and B, respectively. It is observed that, in both cases, the reaction rate (per gram of catalyst) increases with increasing Na or Cs content up to a certain value and then decreases upon further increasing alkali loading. Regarding turnover frequencies, representative results listed in Table 1 show that the highest TOF is obtained for the sample doped with Na:Pt = 1.0. The apparent activation energy of the reaction does not depend strongly on the nature or concentration of the promoter and takes values in the range of 63 to 76 kJ mol^{-1} (Table 1).

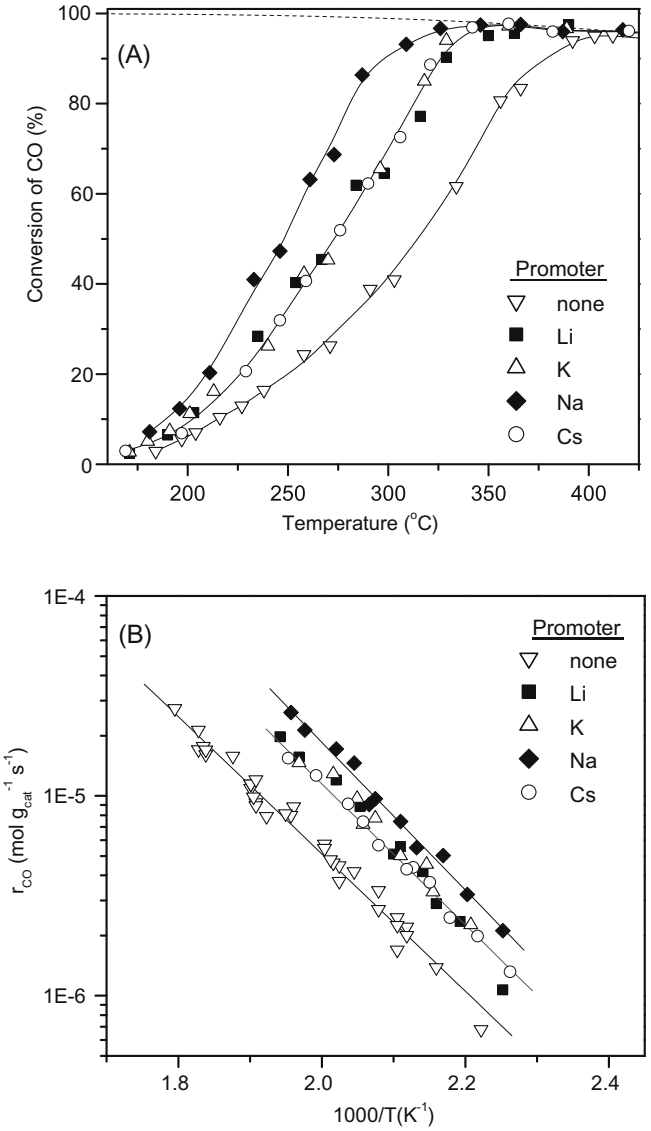

Fig. 4. Effect of alkali promotion on the catalytic performance of $Pt/X–TiO_2$ catalysts of the same alkali:Pt atomic ratio (X:Pt = 1:1). (A) Conversion of CO as function of reaction temperature. Equilibrium CO conversion is shown for comparison (dashed line). (B) Arrhenius plots of reaction rates obtained under differential reaction conditions.

3.3.2. Ru and Pd catalysts

In our previous study of NM/TiO_2 catalysts [22], it was shown that the specific reaction rate (TOF) for the title reaction decreases in the order of Pt > Rh > Ru > Pd, with Pt being about 20 times more active than Pd. In order to investigate the effect of alkali promotion of TiO_2 on the WGS activity of dispersed noble metal catalysts which are less active than Pt, representative catalytic performance tests and kinetic measurements were conducted over selected $Ru/Na–TiO_2$ and $Pd/Cs–TiO_2$ catalysts. In Fig. 7 are shown results obtained for $Ru/Na–TiO_2$ catalysts of variable Na content. It is ob-

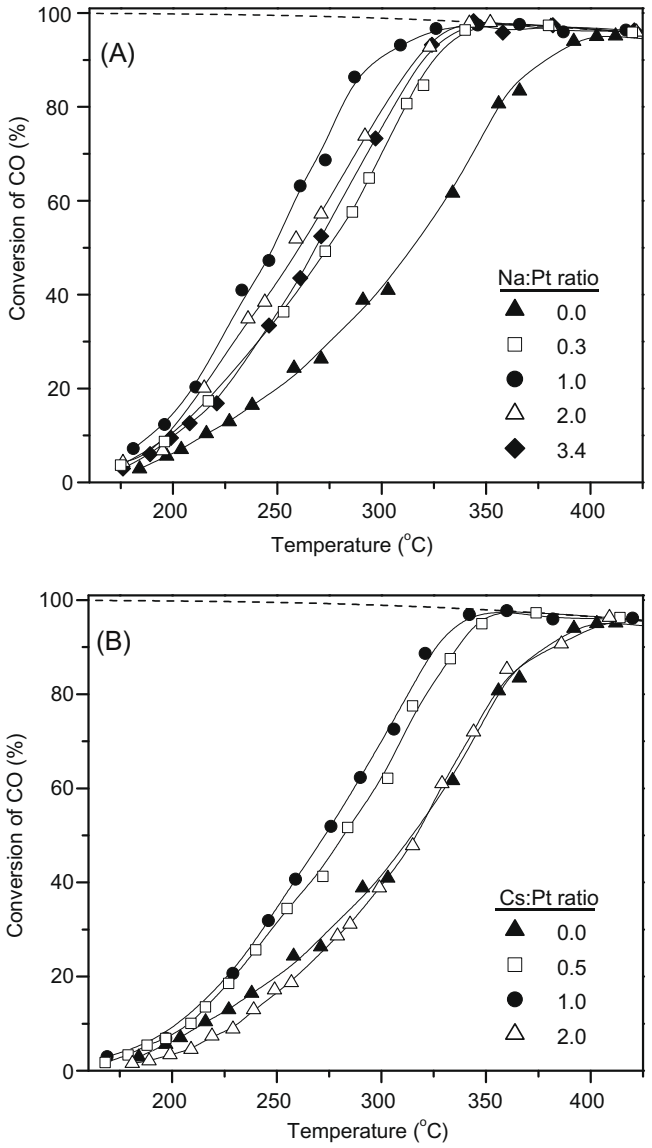

Fig. 5. Effects of (A) sodium and (B) cesium loading, expressed as alkali:Pt atomic ratio, on the catalytic performance of Pt/X–TiO_2 catalysts. Equilibrium CO conversion is shown for comparison (dashed line).

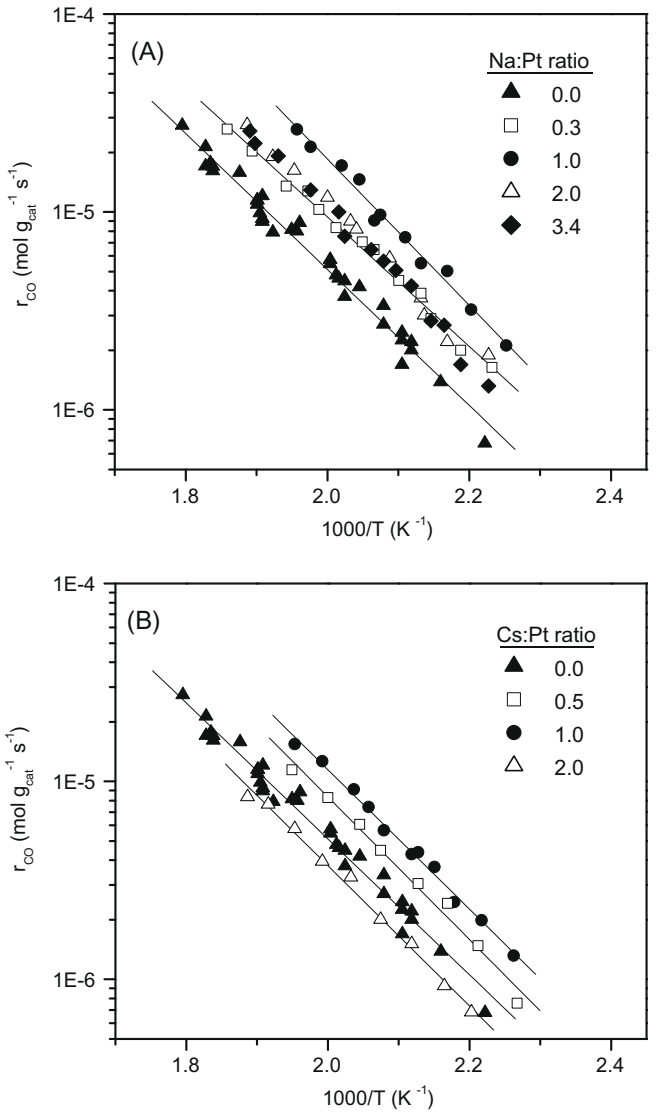

Fig. 6. Arrhenius plots of reaction rates obtained over (A) sodium- and (B) cesium-promoted Pt/X–TiO_2 catalysts.

served that addition of 0.06 wt.% Na (Na:Ru = 0.5) on the TiO_2 support results in a shift of the CO conversion curve toward lower temperatures by *ca.* 60 °C (Fig. 7A) and that the reaction rate (per gram of catalyst) at 250 °C increases by a factor of 4 (Fig. 7B), compared to unpromoted Ru/TiO_2. Further increase of Na:Ru ratio to 1.8 improves catalytic performance slightly. The same trend is observed for TOF (Table 1).

Regarding the least active Pd/TiO_2 catalyst, addition of 0.34 wt.% Cs (Cs:Pd = 0.5) results in a shift of the CO conversion curve toward lower temperatures by *ca.* 45 °C (Fig. 8A) and in an increase in reaction rate by a factor of 3 (Fig. 8B, Table 1). Further increasing Cs:Pd atomic ratio to 1.1 has the opposite effect.

4. Discussion

Results of catalytic performance tests and kinetic measurements (Figs. 4–8 and Table 1) show that the WGS activity of NM/TiO_2 catalysts depends strongly on the type and loading of alkali promoters. A similar, but less pronounced, effect is observed for the apparent activation energy (E_a) of the reaction which, for Pt/Na–TiO_2 catalysts, is generally higher than unpromoted Pt/TiO_2 (Table 1). Qualitatively similar results have been obtained by Yentekakis et al. [43], who investigated reduction of NO by propene over Na-promoted Pd/YSZ catalysts. The authors reported that optimal results were obtained for catalyst promoted with 0.068 wt% Na (Na:Pd = 0.67), the activity of which was about 10 times higher than that of unpromoted Pd/YSZ. This was accompanied by a significant increase in E_a from 84 to 160 kJ mol^{-1} with a concomitant pronounced increase in the pre-exponential factor [43]. Thus, alkali promoters seem to be able to affect both the pre-exponential rate term (frequency factor) and the activation energy of the reaction through the number and strength, respectively, of catalytically active sites.

Results of H_2-TPD experiments presented in Figs. 1–3 indicate that adsorption sites related to the MT peak are those that are most strongly influenced by the presence of the promoters. It is therefore reasonable to suggest that these sites, proposed to be located at the metal-support interface, are the active sites for the WGS reaction. In the following, an attempt is made to explain the present results based on the influence of the promoters on the number and chemisorption strength of these sites.

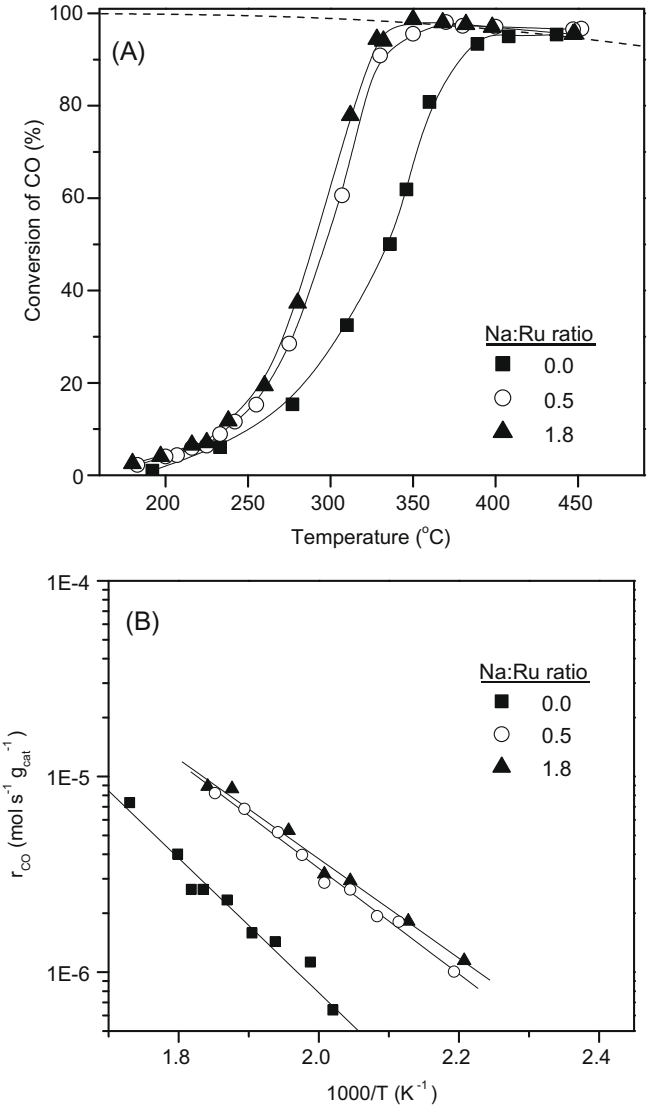

Fig. 7. Effects of Na loading on (A) the catalytic performance and (B) the intrinsic reaction rate of Ru/Na–TiO_2 catalysts.

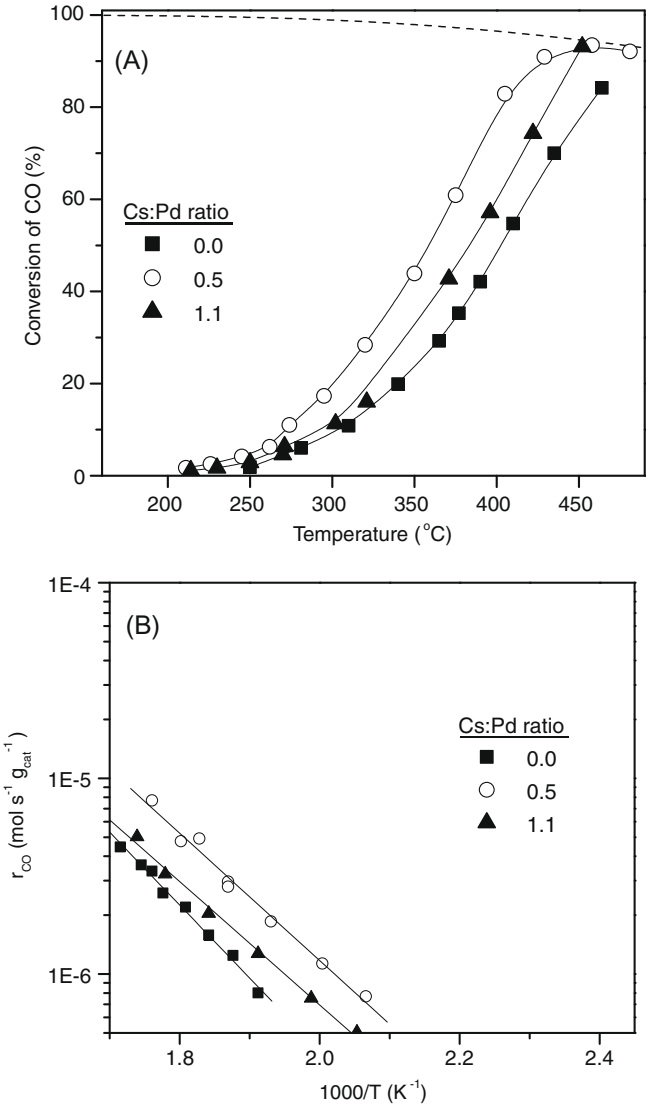

Fig. 8. Effects of Cs loading on (A) the catalytic performance and (B) the intrinsic reaction rate of Pd/Cs–TiO_2 catalysts.

4.1. The nature of catalytically active sites

Results of our previous studies clearly showed that the WGS activity of dispersed noble metal catalysts is closely related to the reducibility of the metal oxide support [22–26]. For instance, activity of Pt and Ru catalysts was found to be 1–2 orders of magnitude higher when supported on "reducible" metal oxides, such as TiO_2 and CeO_2 than "irreducible" metal oxides, such as Al_2O_3 and SiO_2. Regarding the nature of catalytically active sites, results of DRIFTS experiments obtained over Pt/TiO_2 catalyst with the use of CO as probe molecule indicated the existence of a special kind of sites with exceptional electron-donating properties, located at the metal-support interface [26,27]. Based on the results of ^{18}O-isotopic transient experiments, it has been proposed that these sites are of the form of Pt–$\square_s$–Ti^{3+}, where $\square_s$ denotes an oxygen defect vacancy [44]. It is therefore of interest to examine the way that these sites can be created over NM/TiO_2 catalysts and the possible effects of alkali on their number and chemisorption strength.

A prerequisite for the creation of a new type of sites at the metal-support interface (such as Pt–$\square_s$–Ti^{3+}) is interaction of dispersed metal crystallites with the metal oxide support. As discussed in detail by Diebold [45], certain metal atoms (M) deposited on TiO_2 are able to reduce the substrate and themselves become oxidized according to the reaction:

$$M + TiO_2 \rightarrow MO_x + TiO_{2-x} \quad (1)$$

Thermodynamic considerations imply that reaction (1) may take place only when the standard free energy of the oxide (MO_x) formation per mol of oxygen, ΔH_f^o, is more negative than ΔH_f^o of TiO_2 reduction to Ti_2O_3 (or TiO):

$$2TiO_2 \rightarrow 2Ti_2O_3 + \frac{1}{2}\,O_2(g) \quad \Delta H_f^o = 364\ \text{kJ mol}^{-1} \quad (2)$$

The above requirement is satisfied for transition metals on the left side of the periodic table, and also for alkali and alkaline earth metals. In contrast, noble metals such as Pt, Ru, and Pd are not expected to interact strongly with stoichiometric TiO_2 [45].

On the other hand, it is well known that dispersed noble metal crystallites may interact with partly reduced titania support. For instance, results of XPS and UPS experiments obtained over Pt supported on $TiO_2(1\,1\,0)$ showed that a localized electronic charge transfer occurs from Ti^{3+} states to Pt clusters in the presence of surface defects [46]. Thus, the presence of Ti^{3+} species in the close neighborhood of dispersed noble metal crystallites seems to be a

necessary requirement for the creation of a new type of sites at the metal-support interface and for the onset of electronic-type interactions between the metal and the support. Such sites can be created in several ways on the surface of TiO_2, including (i) partial reduction with hydrogen at elevated temperatures, which is related to strong metal-support interactions (SMSI effect), (ii) heat treatment at sufficiently high temperature to remove oxygen from the support, (iii) photochemical reduction, and (iv) deposition of an active metal, such as alkali or alkaline earth metal, according to reaction (1).

Based on the above discussion, the effects of alkali on the chemisorptive and catalytic properties of the present NM/X–TiO_2 catalysts may be understood, at least in part, by considering the reactivity of the alkali promoters toward oxygen of the TiO_2 support. In particular, it is proposed that added alkali interacts strongly with titania thereby leading to partial reduction of TiO_2 (according to reaction (1)) and creation of $\square_s$–Ti^{3+} sites. This argument is supported, for example, by results of Onishi et al. [47] who reported that Na deposited on TiO_2(1 1 0) interacts strongly with surface oxygen atoms thereby causing charge transfer to the substrate and reduction of Ti^{4+} to Ti^{3+}. If this is the case, then noble metal atoms located at the perimeter of dispersed metal crystallites are expected to be influenced indirectly by the presence of the promoter via the creation of NM–$\square_s$–Ti^{3+} sites at the metal-support interface. The observation that added alkali do not affect, practically, the characteristics of the LT H_2-TPD peak (Figs. 1 and 3) implies that the effect is of short-range and does not influence adsorption on the surface of noble metal crystallites, at least in the range of alkali loadings used in the present study. This can be explained by considering that, because of the high relative dielectric constant of TiO_2 (~130), the charge located at the interface will be about 130 times larger than the charge at the free metal surface [48]. If one takes into account the attractive contribution of the positively charged depletion region in the semiconductor, it may be concluded that the charge transfer at the free metal surface will be negligible [48]. This argument is supported by FTIR results of our previous study [27], which showed that the stretching frequency and the relative intensity of bands assigned to linearly adsorbed CO on Pt crystallites (bands at 2089 and 2062 cm^{-1}) are not affected by the presence of added alkali on the TiO_2 support.

4.2. Effects of alkali on the population and chemisorption strength of active sites

The presence of oxygen vacancies on TiO_2 is expected to result in electron transfer from the support to noble metal atoms located in their close vicinity, i.e., at the metal-support interface. This should result in weakening of the adsorption strength of these sites toward electron donors, such as hydrogen, and in strengthening of their adsorption strength toward electron acceptors, such as CO [12]. Results of our present (Figs. 1–3) and previous [27] studies clearly show that this is the case for all NM/X–TiO_2 catalysts investigated.

It is of interest to note here that weakening of the bond strength of hydrogen adsorbed at the metal-support interface with increasing alkali content should be accompanied by a decrease in the population of this species. However, results obtained for Pd/Cs–TiO_2 (Fig. 3A), Ru/Na–TiO_2 (Fig. 3B), and Pt/Cs–TiO_2 [27] catalysts show that this is not the case for low alkali loadings. In particular, the intensity of the MT H_2-TPD peak initially increases with increase of alkali loading, goes through a maximum at a certain X:NM ratio, and then decreases for higher promoter contents (Fig. 3). This provides evidence that the presence of alkali promoters on the support results in the creation of additional adsorption sites at the metal-support interface. It may then be argued that, for low alkali contents, the population of hydrogen adsorbed at the metal-support interface increases due to the creation of a higher amount of $\square_s$–Ti^{3+} defects and, concomitantly, of a higher amount of NM–$\square_s$–Ti^{3+} adsorption sites. However, for higher alkali loadings the amount of adsorbed hydrogen at the metal-support interface decreases due to substantial weakening of the bond strength, which is the case for all NM–X combinations investigated (Fig. 3, and Ref. [27]).

Creation of new active sites at the metal-support interface has been often used to account for the relatively high activity of TiO_2-supported metal catalysts [49,50]. For instance, Bracey and Burch [49], who investigated the activity of Pd/TiO_2 and Pd/SiO_2 catalysts for the CO/H_2 reaction, concluded that the high activity of Pd/TiO_2 is due to the creation of new active sites at the interface between the metal and the support. The authors proposed that the active site is a Ti^{3+} cation exposed in the surface of the support, adjacent to a normal metal particle. It was proposed that these new sites have the capacity to adsorb or assist in the adsorption of CO. Similar conclusions were obtained for Ni/TiO_2 catalysts [50]. Similarly, Marcelin et al. [51], who investigated adsorption of hydrogen over Cs- and Li-promoted Rh/TiO_2 catalysts, proposed that addition of alkalis results either in changes in the energetics of the active sites or in the formation of new sites on the support or at the rhodium–titania interface [51].

Alkali promotion of TiO_2 may be also discussed in terms of strong metal-support interactions (SMSI), first reported by Tauster et al. [52]. The SMSI effect can be induced by high temperature reduction treatment of TiO_2-supported catalysts and is believed to result in (a) creation of exposed Ti^{3+} species, which interact strongly with dispersed metal crystallites, and/or (b) migration of reduced suboxide species on the surface of metal crystallites [52–54]. At low reduction temperatures, the SMSI effect may be considered to be purely electronic [55], i.e., it is not accompanied by decoration of noble metal particles by TiO_x suboxides. In this respect, promotion by alkalis induces the same effects on the properties of NM/TiO_2 catalysts as does reduction temperature in SMSI, i.e., creation of $\square_s$–Ti^{3+} defects. The number of these sites may be controlled by varying either dopant content (alkali promotion) or reduction temperature (SMSI). Thus, the observed effect of alkali on the chemisorptive and catalytic properties of NM/TiO_2 catalysts may be viewed as a "permanent" SMSI effect, which can be used to manipulate the number and chemisorption strength of sites located at the metal-support interface.

4.3. The volcano-type dependence of WGS activity on alkali loading

In practically all noble metal–alkali combinations investigated here, the reaction rate initially increases with increase of promoter loading, goes through a maximum at a certain dopant level, and then decreases for higher alkali contents (Figs. 5–8 and Table 1). A similar dependence of catalytic activity on alkali loading has been reported in several studies [8,9,43]. For instance, Kazi et al. [8] reported that the rate of CO hydrogenation over Li-doped Pd/SiO_2 catalysts increases by a factor of 2 for samples with Li:Pd ratio of 1, relative to the unpromoted catalyst, but higher levels of Li (Li:Pd $\geqslant$ 2) give reduced activities [8]. Huang et al. [9], who investigated CO methanation over alkali-promoted Ni/SiO_2-Al_2O_3 catalysts, found that TOF increases with increase of Na content and passes through a maximum at 0.2% Na with an enhancement by a factor of 6, compared to the sodium-free catalyst. The suppression of the promoting effect at higher Na levels has been attributed to a kind of "poisoning effect" induced by the alkali, either directly via the metal or metal-support interface, or indirectly via the support itself [9]. A volcano-type dependence of the reaction rate on sodium loading has also been reported by Yentekakis et al. [43], who investigated reduction of NO by propene over Pd/YSZ cata-

lysts. The presence of a maximum in the reaction rate has been attributed to poisoning due to site-blocking above some optimum alkali loading (0.068 wt% Na) [43].

The volcano-type dependence of reaction rate on alkali loading, which is often observed for chemically and electrochemically promoted catalytic materials, can be understood by taking into account the effects of the promoter on the chemisorptive bonds of electron donor and electron acceptor adsorbed species [56]. Regarding the WGS reaction, Grenoble et al. [57] found that a volcano-type relation exists between activity of Al_2O_3-supported metal catalysts and their respective CO heats of adsorption. In this respect, it is tempting to examine if such a correlation exists between the adsorption strength of NM–$\square_s$–Ti^{3+} sites toward CO and the WGS activity of NM/X–TiO_2 catalysts. For this purpose, one may use the desorption temperature of the MT H_2-TPD peak, which provides a measure of the adsorption strength of active sites toward hydrogen. It should be reminded here that, although chemisorption strength toward hydrogen decreases with increase of alkali loading (Figs. 1–3), the opposite is true for CO adsorption [27].

In Fig. 9 is plotted the turnover frequency of CO conversion at 250 °C (data taken from Table 1) as a function of T_{max} (data taken from Fig. 2) for Pt/X–TiO_2 catalysts (X = Li, Na, K, Cs) of variable alkali loading. It is observed that reaction rate exhibits a volcano-type dependence on the chemisorption strength of Pt–$\square_s$–Ti^{3+} sites toward hydrogen. In particular, addition of small amounts of alkali, which results in weakening of hydrogen adsorption strength (and therefore strengthening of the CO adsorption strength), results in an increase of the WGS reaction rate. For higher amounts of alkali promoters, the chemisorption strength of Pt–$\square_s$–Ti^{3+} sites for hydrogen (CO) is further decreased (increased), but this results in catalysts with lower activity. As a result, specific reaction rate goes through a maximum for catalysts containing 0.06 wt.% Na or 0.10 wt.% K, which exhibit an intermediate strength for hydrogen (and CO) adsorption. In both cases, the alkali:Pt atomic ratio is equal to 1 (Table 1). It is of interest to note that data obtained for all different types and loadings of alkali promoters fall on the same curve, implying that the rate is determined to a large extent by the chemisorptive properties of sites at the metal-support interface. Thus, results of Fig. 9 are qualitatively similar to those reported by Grenoble et al. [57] over M/Al_2O_3 catalysts. The difference is that Grenoble et al. altered the strength of CO chemisorption by varying the nature of the dispersed metallic phase, whereas in the present study this has been achieved by varying the nature and/or loading of alkali promoters on the TiO_2 support.

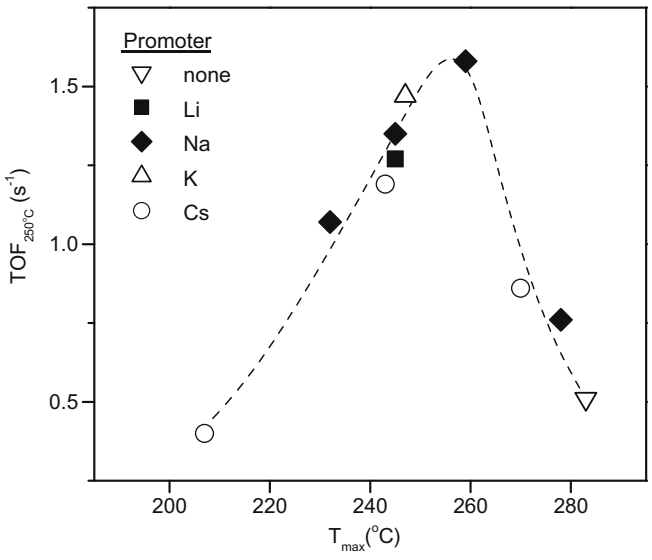

Fig. 9. Volcano-type dependence of turnover frequency at 250 °C on the desorption temperature (T_{max}) of the medium temperature (MT) peak observed in H_2-TPD profiles of Pt/X–TiO_2 catalysts (X = Li, K, Na, Cs).

4.4. Mechanistic implications

The mechanistic schemes proposed so far for the WGS reaction over metal oxide-supported NM catalysts can be divided into two broad categories, namely, redox and associative [58]. Redox mechanisms involve production of CO_2 via oxidation of CO adsorbed at the metal-support interface with an oxygen atom of the support, which is subsequently reoxidized by H_2O to liberate H_2 [59–61]. Associative mechanisms involve steps where CO adsorbed on the noble metal interacts with hydroxyl groups of the support to form an intermediate species (e.g. formate) which further decomposes to CO_2 and H_2 [62–64]. A hybrid mechanism, the so called "associative formate route with redox regeneration" of the oxide support, has also been proposed [65–67], in which conversion of surface formate to H_2 and CO_2 occurs using oxygen from the support and not from water.

It is important to note that all mechanistic schemes involve bifunctional catalysis, in the sense that the noble metal activates CO whereas the metal oxide adsorbs and activates H_2O [58–67]. In this respect, it is of interest to note that NM–$\square_s$–Ti^{3+} sites fulfill the requirement for catalyzing this dual site process, since they may be involved in adsorption/activation of both CO and H_2O. Regarding water, the presence of surface defects on the TiO_2 support seems to be a prerequisite for its activation via defect-induced water dissociation [68–70]. For instance, results of STM experiments and DFT calculations [68,69] showed that, at low coverage, water dissociation on the rutile (1 1 0) surface occurs exclusively on oxygen vacancies in the surface layer. These vacancies have been shown to dissociate H_2O through the transfer of one proton to a nearby oxygen atom, forming two hydroxyl groups for every vacancy. Similar results have been reported for the most stable anatase (1 0 1) surface [70], for which first-principles molecular-dynamic simulations showed the existence of a mechanism for thermodynamically favored spontaneous dissociation of water at low coverages of oxygen vacancies. It was concluded that it is likely that all water molecules near vacancy sites are dissociated at low coverages [70]. The amount of water dissociation has been found to be limited by the density of oxygen vacancies present on the clean surface [69]. Thus, alkali-induced creation of $\square_s$–Ti^{3+} sites should enhance the capacity of titania toward dissociative adsorption of water. The presence of oxygen vacancies adjacent to a metal particle provides the necessary dual-function NM–$\square_s$–Ti^{3+} sites required for the WGS reaction to proceed.

It should be noted that NM–$\square_s$–Ti^{3+} sites can also be formed in the absence of alkali promoters because, under the reducing environment of the WGS reaction, dispersed noble metals may reduce the surface of TiO_2 effectively. The same is true for other reducible metal oxides supports. For instance, recent studies conducted over Pt/CeO_2 and Au/CeO_2 catalysts [71–73] indicate that the role of the dispersed metallic phase is not only restricted in providing sites for CO adsorption, but also in modifying the properties of the support by creating new active sites at the metal-support interface, namely, oxygen vacancies within the support or partially reduced sites at the metal-support interface. Jacobs et al. [64] recognized that, for Pt/CeO_2 catalysts, partial reduction of ceria is a necessary step in both the redox and the formate mechanisms. In the formate mechanism, the reduction of ceria surface shell is necessary to generate the bridging OH group active sites, whereas in the redox mechanism, reduction of ceria is directly involved in the reaction mechanism [64]. Finally, Lefferts et al. [65–67] showed that the WGS reaction proceeds over Pt/TiO_2 catalysts via both the redox route

and the associative formate route with redox regeneration, both of which require the presence of oxygen vacancies on the support. That is, water activation can occur by both hydroxyl formation and redox water splitting on oxygen vacancies present on the reduced TiO_2 surface. The role of water is related to regeneration of hydroxyl groups and simultaneous re-oxidation of TiO_2 [65–67].

5. Conclusions

The chemisorptive properties and WGS-activity of NM/TiO_2 catalysts (NM = Pt, Ru, Pd) can be modified appreciably by addition of small amounts of alkalis (X = Li, Na, K, Cs) on the TiO_2 support prior to dispersion of the noble metal. Added alkalis interact strongly with the TiO_2 surface and result in the creation of $\square_s$–Ti^{3+} defects which, in turn, affect the chemisorptive properties of NM atoms located at the metal-support interface. The so formed NM–$\square_s$–Ti^{3+} sites are proposed to be the catalytically active sites for the WGS reaction, since they are capable of adsorption and activation of both CO and H_2O. Increasing alkali loading results in an increase of the number of these sites and in a monotonic decrease (increase) of their adsorption strength toward hydrogen (carbon monoxide). A volcano-type relation exists between the turnover frequency of CO and the chemisorption strength of NM–$\square_s$–Ti^{3+} sites toward hydrogen (or CO). Optimal results are obtained for Na-promoted Pt/TiO_2 catalysts with Na:Pt = 1:1, the specific activity (TOF) of which is about three times higher, compared to that of the unpromoted catalyst. The effects of alkali promotion on the chemisorptive and catalytic properties of NM/TiO_2 catalysts may be described as a "permanent" SMSI effect.

References

[1] M. Konsolakis, I.V. Yentekakis, Appl. Catal. B. 29 (2001) 103.
[2] M. Konsolakis, I.V. Yentekakis, A. Palermo, R.M. Lambert, Appl. Catal. B 33 (2001) 293.
[3] G. Goula, P. Katzourakis, N. Vakakis, T. Papadam, M. Konsolakis, M. Tikhov, I.V. Yentekakis, Catal. Today 127 (2007) 199.
[4] S.S. Mulla, N. Chen, L. Cumaranatunge, W.N. Delgass, W.S. Epling, F.H. Ribeiro, Catal. Today 114 (2006) 57.
[5] G. Avgouropoulos, E. Oikonomopoulos, D. Kanistras, T. Ioannides, Appl. Catal. B 65 (2006) 62.
[6] H. Tanaka, S.-I. Ito, S. Kameoka, K. Tomishige, K. Kunimori, Appl. Catal. A 250 (2003) 255.
[7] C. Pedrero, T. Waku, E. Iglesia, J. Catal. 233 (2005) 242.
[8] A.M. Kazi, B. Chen, J.G. Goddwin Jr., G. Marcelin, N. Rodriguez, R.T.K. Baker, J. Catal. 157 (1995) 1.
[9] C.P. Huang, J.T. Richardson, J. Catal. 51 (1978) 1.
[10] H.N. Evin, G. Jacobs, J. Ruiz-Martinez, G.A. Thomas, B.H. Davis, Catal. Lett. 120 (2008) 166.
[11] J.M. Pigos, C.J. Brooks, G. Jacobs, B.H. Davis, Appl. Catal. A 328 (2007) 14.
[12] C.G. Vayenas, S. Bebelis, C. Pliangos, S. Brosda, D. Tsiplakides, Electrochemical Activation of Catalysis, Kluwer Academic Publishers/Plenum Press, New York, 2001.
[13] F.J. Williams, M.S. Tikhov, A. Palermo, N. Macleod, R.M. Lambert, J. Phys. Chem. B 105 (2002) 2800.
[14] F. Dorado, A. de Lucas-Consuegra, P. Vernoux, J.L. Valverde, Appl. Catal. B 73 (2007) 42.
[15] Ch. Karavasilis, S. Bebelis, C.G. Vayenas, J. Catal. 160 (1996) 205.
[16] A. de Lucas-Consuegra, F. Dorado, J.L. Valverde, R. Karoum, P. Vernoux, J. Catal. 251 (2007) 474.
[17] I.V. Yentekakis, G. Moggridge, C.G. Vayenas, R.M. Lambert, J. Catal. 146 (1994) 292.
[18] H.P. Bonzel, A.M. Bradshaw, G. Ertl (Eds.), Physics and Chemistry of Alkali Metal Adsorption, Elsevier, Amsterdam, 1989.
[19] D. Heskett, Surf. Sci. 199 (1988) 67.
[20] H.P. Bonzel, Surf. Sci. Rep. 8 (1987) 43.
[21] D.L. Trimm, Z.I. Önsan, Catal. Rev. 43 (2001) 31.
[22] P. Panagiotopoulou, D.I. Kondarides, J. Catal. 225 (2004) 327.
[23] P. Panagiotopoulou, D.I. Kondarides, Catal. Today 112 (2006) 49.
[24] P. Panagiotopoulou, D.I. Kondarides, Catal. Today 127 (2007) 319.
[25] P. Panagiotopoulou, J. Papavasiliou, G. Avgouropoulos, T. Ioannides, D.I. Kondarides, Chem. Eng. J. 134 (2007) 16.
[26] P. Panagiotopoulou, A. Christodoulakis, D.I. Kondarides, S. Boghosian, J. Catal. 240 (2006) 114.
[27] P. Panagiotopoulou, D.I. Kondarides, J. Catal. 260 (2008) 141.
[28] K. Foger, J.R. Anderson, J. Catal. 54 (1978) 318.
[29] P.G. Menon, G.F. Froment, J. Catal. 59 (1979) 138.
[30] O. Alexeev, D.-W. Kim, G.W. Graham, M. Shelef, B.C. Gates, J. Catal. 185 (1999) 170.
[31] J.T. Miller, B.L. Meyers, F.S. Modica, G.S. Lane, M. Vaarkamp, D.C. Koningsberger, J. Catal. 143 (1993) 395.
[32] F. Benseradj, F. Sadi, M. Chater, Appl. Catal. B 228 (2002) 135.
[33] D.I. Kondarides, X.E. Verykios, J. Catal. 174 (1998) 52.
[34] J. Rieck, A. Bell, J. Catal. 103 (1987) 46.
[35] B. Ngamsom, N. Bogdanchikova, M.A. Borja, P. Praserthdam, Catal. Commun. 5 (2004) 243.
[36] V.H. Sandoval, C.E. Gigola, Appl. Catal. A 148 (1996) 81.
[37] C.-C. Hong, C.-T. Yeh, Mater. Chem. Phys. 20 (1988) 471.
[38] H.-Y. Lin, Y.-W. Chen, Thermochim. Acta 419 (2004) 283.
[39] J.C. Conesa, J. Soria, J. Phys. Chem. 86 (1982) 1392.
[40] K.G. Azzam, I.V. Babich, K. Seshan, L. Lefferts, Appl. Catal. A 338 (2008) 66.
[41] Y.T. Kim, E.D. Park, H.C. Lee, D. Lee, K.H. Lee, Appl. Catal. B 90 (2009) 45.
[42] X. Zhu, T. Hoang, L.L. Lobban, R.G. Mallinson, Catal. Lett. 129 (2009) 135.
[43] I.V. Yentekakis, R.M. Lambert, M.S. Tikhov, M. Konsolakis, V. Kiousis, J. Catal. 176 (1998) 82.
[44] C.M. Kalamaras, P. Panagiotopoulou, D.I. Kondarides, A.M. Efstathiou, J. Catal. 264 (2009) 117.
[45] U. Diebold, Surf. Sci. Rep. 48 (2003) 53.
[46] K.D. Schierbaum, S. Fischer, M.C. Torquemada, J.L. de Segovia, E. Román, J.A. Martín-Gago, Surf. Sci. 345 (1996) 261.
[47] H. Onishi, T. Aruga, C. Egawa, Y. Iwasawa, Surf. Sci. 199 (1988) 54.
[48] T. Ioannides, X.E. Verykios, J. Catal. 161 (1996) 560.
[49] J.D. Bracey, R. Burch, J. Catal. 86 (1984) 384.
[50] R. Burch, A.R. Flambard, J. Catal. 85 (1984) 16.
[51] G. Marcelin, J.E. Lester, S.F. Mitchell, J. Catal. 102 (1986) 240.
[52] S.J. Tauster, S.C. Fung, R.L. Garten, J. Am. Chem. Soc. 100 (1978) 170.
[53] S. Bernal, J.J. Calvino, M.A. Cuqui, J.M. Catica, C. Larese, J.A. Pérez Omil, J.M. Pintado, Catal. Today 50 (1999) 175.
[54] G.L. Haller, D.E. Resasco, Adv. Catal. 36 (1989) 173.
[55] J.P. Belzunegui, J. Sanz, J.M. Rojo, J. Am. Chem. Soc. 112 (1990) 4066.
[56] C.G. Vayenas, S. Brosda, C. Pliangos, J. Catal. 203 (2001) 329.
[57] D.C. Grenoble, M.M. Estadt, D.F. Ollis, J. Catal. 87 (1981) 90.
[58] J. Barbier Jr., D. Duprez, Appl. Catal. B 3 (1993) 61.
[59] H. Cordatos, T. Bunluesin, J. Stubenrauch, J.M. Vohs, R.J. Gorte, J. Phys. Chem. 100 (1996) 785.
[60] S. Hilaire, X. Wang, T. Luo, R.J. Gorte, J. Wagner, Appl. Catal. A 215 (2001) 271.
[61] Y. Li, Q. Fu, M. Flytzani-Stephanopoulos, Appl. Catal. B 27 (2000) 179.
[62] T. Shido, Y. Iwasawa, J. Catal. 141 (1993) 71.
[63] G. Jacobs, L. Williams, U. Graham, G.A. Thomas, D.E. Sparks, B.H. Davis, Appl. Catal. A 252 (2003) 107.
[64] G. Jacobs, P.M. Patterson, U.M. Graham, A.C. Crawford, B.H. Davis, Int. J. Hydrogen Energy 30 (2005) 1265.
[65] K.G. Azzam, I.V. Babich, K. Seshan, L. Lefferts, J. Catal. 251 (2007) 153.
[66] K.G. Azzam, I.V. Babich, K. Seshan, L. Lefferts, Appl. Catal. B 80 (2008) 129.
[67] P.O. Graf, D.J.M. de Vlieger, B.L. Mojet, L. Lefferts, J. Catal. 262 (2009) 181.
[68] I.M. Brookes, C.A. Muryn, G. Thornton, Phys. Rev. Lett. 87 (2001) 266103.
[69] R. Schaub, P. Thostrup, N. Lopez, E. Laegsgaard, I. Stensgaard, J.K. Norskov, F. Besenbacher, Phys. Rev. Lett. 87 (2001) 266104.
[70] A. Tilocca, A. Selloni, J. Chem. Phys. 119 (2003) 7445.
[71] Q. Fu, H. Saltsburg, M. Flytzani-Stephanopoulos, Science 301 (2003) 935.
[72] Q. Fu, W. Deng, H. Saltsburg, M. Flytzani-Stephanopoulos, Appl. Catal. B 56 (2005) 57.
[73] A. Goguet, F. Meunier, J.P. Breen, R. Burch, M.I. Petch, A.F. Chenciu, J. Catal. 226 (2004) 382.